INTERNATIONAL JOURNAL OF OPTIMIZATION IN CIVIL ENGINEERING
Int. J. Optim. Civil Eng., 2023; 13(2):155-176

AN ADAPTIVE-BAND STRATEGY TO ACCELERATE DISCRETE OPTIMIZATION OF SPACE TRUSS STRUCTURES

M. Shahrouzi[*, †] and A. Salehi
Civil Engineering Department, Faculty of Engineering, Kharazmi University, Tehran, Iran

[DOI: 10.22068/ijoce.2023.13.2.547]

ABSTRACT

In most practical cases, structural design variables are linked to a discrete list of sections for optimal design. Cardinality of such a discrete search space is governed by the number of alternatives for each member group. The present work offers an adaptive strategy to detect more efficient alternatives and set aside redundant ones during optimization. In this regard, the difference between the lower and the upper bounds on such variables is gradually reduced by a procedure that adapts history of the selected alternatives in previous iterations. The propsed strategy is implemented on a hybrid paritcle swarm optimizer and imperialist competitive algorithm. The former is a basic swarm intelligent method while the later utilizes subpopulations in its search. Spatial and large-scale structures in various shapes are treated showing successive performance improvement. Variation of a diversity index and resulting band size are traced and discussed to declare behavior merits of the proposed adaptive band strategy.

Keywords: Adaptive-band sizing; discrete structural optimization; truss; swarm intelligence; imperialist competitive algorithm; efficiency improvement.

Received: 14 October 2022; Accepted 12 December 2022

1. INTRODUCTION

Several real-world applications deal with optimal design under engineering constraints [1]. Structural optimization particularly by minimizing its material consumption has been an active field of research since early 1900's [2–4]. The problem has already been extended to various types of structures in presence of their specific constraints. They include sizing design of frame and truss structures [5,6], geometry assessment and topology optimization

[*]Corresponding author: Civil Engineering Department, Faculty of Engineering, Kharazmi University, Tehran & Karaj, Iran
[†]E-mail address: shahruzi@khu.ac.ir (Mohsen Shahrouzi)

of structures under static or dynamic constraints [7,8]. Metaheuristic algorithms are popular tools to solve such optimization problems as they utilize clear concepts and gradient-free operators to overpass local optima toward global optimum [9].

Spatial structures are considered practical solutions to cover large spans. Majority of them consist of axial members pin-jointed to each other in modular manner and some can be modeled and efficiently analyzed using the concepts of symmetry. Large number of structural members/nodes subjected to stress/deflection limits, is a practical challenge for their sizing optimization [10,11]. Many these models fall in the category of large-scale structures [12]. In order to evaluate behavior constraints for every design alternative, the whole structural model should be analyzed that exerts computational burden to the search process [13]. The more cardinality, the less efficiency and accuracy is expected in finding global optimum [14]. Particularly, the number of available cross-sections, assignable to each member group, governs cardinality of the search space in such a discrete optimization.

In the sizing design problem, there is a direct relation between section areas of the structural members and resulting total weight: by increasing the member area the objective function is expected to be increased. Thus, it may be helpful to sort available sections in ascending order of their areas and classify the corresponding search space as an orderable one [15].

A number of investigators have applied the cross-section ordering in their optimization procedure for structural sizing design. A general framework is offered in [15] that employs some fuzzy membership functions and the trial update strategy from ant colony algorithms [16]. It updates and utilizes an ordered matrix of section indices based on good experiences during the search, utilizing a fuzzy approach. *Adaptive Dimensional Search* [17] is a population-based heuristic that employs evolutionary strategies together with a parameter to control exploration-exploitation balance due to real-time changes on the best experience during the search. The idea is based on sensitivity of the penalized objective function on sizing variables.

As the structural constraints in the penalized objective function should be evaluated by numerical analysis; this type of problem is most suited to zero-order methods such as meta-heuristic algorithms. The present study concerns *Particle Swarm Optimization,* PSO [18] and *Imperialist Competitive Algorithm,* ICA [19] as two well-studied methods in this category. The former is a basis of swarm intelligent algorithms while the latter applies its particular method of generating mixing and collapsing subpopulations. A hybrid variant of ICA and PSO is utilized with less control parameters than both. Then, the proposed variable-band strategy is applied on such an enhanced optimization framework to evaluate its performance improvement in sizing design of spatial structures.

2. STRUCTURAL OPTIMIZATION WITH DISCRETE SIZING VARIABLES

During sizing optimization of a structure, its member areas are updated by selecting from a discrete list of available sections. Suppose that such a list for every q^{th} member group, includes S_q sections, sorted in ascending order of their areas. The optimization problem can thus be formulated as:

[DOI: 10.22068/ijoce.2023.13.2.547]

$$
\begin{aligned}
&\textit{Find}\quad X =< x_1,...,x_D > \\
&\textit{To Minimize}\quad w(X) = \rho \sum_{q=1}^{D} \sum_{i=1}^{n_q} L_i A_i \\
&S.t. \\
&g_j^{\sigma}(\mathrm{X}) : SR_j - 1 \le 0 \\
&g_k^{d}(\mathrm{X}) : DR_k - 1 \le 0 \\
&x_q \in \{x_q^L, x_q^L + 1, x_q^L + 2, ..., x_q^U\},\ q = 1,...,\mathrm{D}
\end{aligned}
\tag{1}
$$

L_i and A_i stand for the length and area of the i^{th} member in the q^{th} group (with n_q members), respectively. ρ is the material density. The structural constraints on the j^{th} member stress and the k^{th} nodal displacement are denoted by $g_j^{\sigma}(\mathrm{X})$ and $g_k^{d}(\mathrm{X})$, respectively. DR_k stands for the corresponding nodal *Displacement Ratio* over its prescribed limit. In case of applying *Allowable Stress Design*; SR_j denotes the ratio of the resulted stress in any j^{th} element over its allowable value.

For every q^{th} group, the lower and upper bounds on section indices are initiated by the integer numbers: $x_q^L = 1$ and $x_q^U = S_q$. Using an exterior penalty approach, such a formulation is transformed to unconstrained form in order to maximize the corresponding fitness as:

$$\textit{Maximize } Fit(X) = -w(X) \times (1 + K_P . \sum_{l} \max(g_l, 0)) \tag{2}$$

where $g_l(X)$ stands for the l^{th} behavior constraint and K_P stands for the penalty factor.

3. PARTICLE SWARM OPTIMIZER

Since Particle Swarm Optimizer was introduced in 1995 as the pioneering method on swarm intelligent computation, it has applied to several engineering problems [20]. In its standard form, PSO can partially simulate movement strategies in a bird flock. In every new instant of time (iteration of the algorithm), an artificial bird (a particle) can move in its previous direction (inertial action) or toward the best of its own experience (cognitive action) or follow the best position already found by the entire swarm (social action). All these actions are integrated in PSO via the following relations to update velocity and position of the corresponding particle:

$$X_i^{t+1} = X_i^t + V_i^{t+1} \tag{3}$$

$$V_i^{t+1} = c_w V_i^t + rand \times c_c \times (P_i^t - X_i^t) + rand \times c_s \times (B^t - X_i^t) \tag{4}$$

[DOI: 10.22068/ijoce.2023.13.2.547]

At the iteration *t*, X_i^t and V_i^t stand for position and velocity of the i^{th} particle, respectively. P_i^t is its best experience while B^t denotes the global best position. The corresponding scale factors for the inertial, cognitive and social terms are represented by c_w, c_c, c_s. The function *rand* adds extra stochastic feature to the algorithm by generating random numbers within [0, 1]. PSO initiates with a population of randomly positioned particles and then for a prescribed number N_I iterates in a loop that updates their positions due to Eq. (3) and Eq. (4). Then, the updated B^t is announced as the optimum.

4. IMPERIALIST COMPETITIVE ALGORITHM

Imperialist Competitive Algorithm, is a population-based metaheuristic method inspired by interaction of some artificial *empires* [19]. According to ICA terminology, every solution vector in the population is called a *country*. The countries within each empire (sub-population) are called *colonies* except their fittest one that is distinguished as the *imperialist*. The power (or fitness) of a country is an inverse measure of its normalized cost. Every imperialist absorbs its colonies during movements within the corresponding empire; meanwhile if one colony gets better than its imperialist they will exchange their role. Once total power of each empire is calculated by fitness of the imperialist plus the scaled mean fitness of its colonies, the empires compete to take possession of colonies from each other. In another word, colonies migrate from weaker empires to the stronger ones. Consequently, weaker empires may become empty and collapse while stronger ones enlarge. The process continues until the strongest imperialist hopefully conquers all the others and just one empire remains. Once the termination criterion is satisfied, the strongest imperialist among the entire population is announced as the optimal design. A simple description of the algorithm can be briefed via the following steps:

Step 1. Initiate N_{emp} empires with randomly positioned colonies. Evaluate fitness of all N_P members of the entire population. Distinguish the fittest vector within every e^{th} empire as its imperialist; denoted by X_{imp}^e.

Step 2. For each empire *e* do:

- Move every c^{th} colony of the empire toward the imperialist by Eq. (5) using a parameter β:

$$X_{c,new}^e = h(X_c^e + (\beta \times rand - 1) \times (X_{imp}^e - X_c^e)) \tag{5}$$

- Evaluate fitness of the new vector and if $X_{c,new}^e$ is fitter than the current X_c^e, replace them. The function $h(.)$ fixes new design vector within its bounds; i.e. $X^L \sim X^U$.
- Update the imperialist as the fittest member of the empire.

Step 3. Perform competition between the empires:

[DOI: 10.22068/ijoce.2023.13.2.547]

- Compute total fitness of the empire by Eq. (6) using the prescribed factor ξ :

$$TF_e = Fit(X_{imp}^e) + \xi . \underset{c}{mean}(Fit(X_c^e)) \tag{6}$$

- Compute power of the empire by:

$$P_e = \frac{TF_e - Q}{\sum_{e=1}^{N_e}(TF_e - Q)} \tag{7}$$

where Q is the maximum total fitness over the empires.

- Migrate the weakest colony (the least fit) from the empire with the least power to the strongest empire that has the most likelihood (power) to possess it.

Step 4. Collapse any empty empire if there exists.

Step 5. Check termination criterion: If the number of iterations has not reached its prescribed limit: N_{Iter} then repeat the main loop from **Step 2**; otherwise announce the strongest imperialist as the optimum. As an alternative termination criterion; a maximum number of fitness evaluations can be set in such a process to $NFE_{\max}$. In the present study extra control parameters are set to $N_{emp} = 0.25N_P$, $\beta = 4$ and $\xi = 0.5$.

5. ADAPTIVE-BAND STRATEGY IN THE PROPOSED ALGORITHM

Many population-based meta-heuristics, can show a decreasing trend of diversity vs iteration so that at final iterations, the velocity vectors approach zero; that is when no further violation about the already-found optimum design is intended. In such a process, the population vectors concentrate more and more on the optimum solution up to final convergence.

Fig.1 illustrates history of some variables' bounds in a sample sizing optimization, provided that a sorted list of structural sections is used. Although traces are not targeted at the same point for different variables, they show a common trend: the bandwidth between lower to upper bounds on section indices, decreases as the iteration number increases. It is also observed that fluctuation of each design variables about its optimum (target) value approaches zero near final iterations.

The phenomenon is particularly useful on orderable search spaces such as those in discrete structural sizing problem [15]. Applying sorted discrete list of sections, the range of variation at every sizing variable hopefully reduces with time (iteration), with respect to the initial lower-to-upper bounds.

In the other hand, lack of search refinement and computational efficiency are practical challenges in sizing design of large-scale structures with many members and several behavior constraints. It motivates the need for efficient solutions in such a design optimization.

[DOI: 10.22068/ijoce.2023.13.2.547]

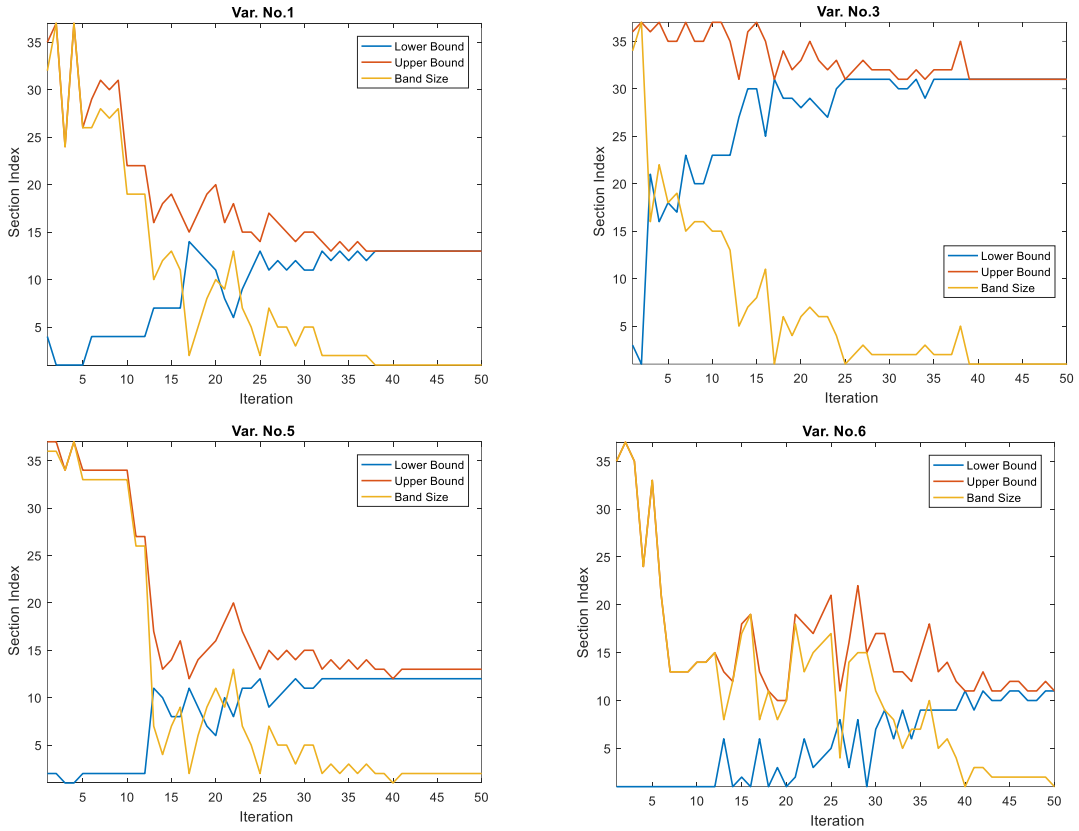

Figure 1. Variation of band size and bounds on design variables during a sizing optimization

Let's call the current range of lower-to-upper bounds for each sizing variable as its *Band Size*, BS. Regarding the aforementioned phenomenon, a strategy is developed for adaptive control of BS, based on tracing positions of every search agent in some previous iterations. It offers adaptive reduction of BS by the following subroutine:

- Record trace of the section indices that have been chosen during optimization; form the iteration, *t-k+1*, up to the current iteration, *t*.
- For every q^{th} sizing design variable do:
  - Identify the minimum and maximum chosen indices as ${}^{t}x_q^L$ and ${}^{t}x_q^U$, respectively.
  - Apply new lower and upper bounds in Eq. (1) by substituting them instead of using original x_q^L and x_q^U, respectively.

The above subroutine can be inserted before/after a walking step in the main algorithm. It applies an *Adaptive Band Size,* ABS to reduce cardinality of the search space and improve the search refinement. Consequently, the proposed *Adaptive Band hybrid Swarm and Imperialist Competition Algorithm,* ABSICA, is revealed via the following steps:

[DOI: 10.22068/ijoce.2023.13.2.547]

Step 1. Initiate k and $\alpha \leftarrow \alpha_0$. Initiate and evaluate the population, then divide it into N_e empires.

Step 2. For every empire *e* do

- For every c^{th} colony of the empire do
  - Generate candidate solution by Eq. (5), exchange with the current if fitter.
- Update the imperialist of the empire

Step 3. Competition between the empires

- Compute total fitness of the empire by Eq. (6)
- Compute power of the empire by Eq. (7)
- Migrate the weakest colony to the strongest empire

Step 4. Collapse any empty empire

Step 5. If the number of fitness evaluations has just reached $\alpha \times NFE_{\max}$ then:

- Update lower/upper bounds on design variables by ABS subroutine.
- Apply the new bounds in the fixing function $h(.)$
- For every i^{th} individual in the population:
  - Move the individual to the new position $x_i^{t,new}$ by:

$$X_i^{t,new} = h(X_i^t + rand \times (P_i^t - X_i^t) + rand \times (B^t - X_i^t)) \tag{8}$$

  - The term P_i^t is the previous best and B^t denotes the global best particle as described in PSO by Eq. (4).
  - Construct a random design vector $x_i^{t,ABS}$ within the updated bounds
  - Move the individual toward $x_i^{t,ABS}$ provided that it is fitter than the current position of the individual; otherwise remain x_i^t unchanged.

$$X_i^{t,new} = h(X_i^t + rand \times (X_i^{t,ABS} - X_i^t)) \tag{9}$$

  - Update α by replacing $\alpha \leftarrow 1.5\alpha$

Step 6. Set back to the original variable bounds for the fixing function $h(.)$

Step 7. If the termination criterion is not satisfied go back to **Step 2**; otherwise announce the optimum.

ABS strategy can be applied to the main algorithm using two parameters; k and α .The integer *k* is the number of recent iterations covered in tracing history of variable bounds. By the rate α, frequency of ABS activation is controlled during the search to prevent the algorithm from premature convergence. Since Eq. (8) is extracted from cognitive and social terms of Eq. (4), it hybridizes such PSO operators with ICA.

[DOI: 10.22068/ijoce.2023.13.2.547]

6. NUMERICAL SIMULATION

The proposed algorithms are applied on a number of spatial truss structures with various shapes. Each example is solved via independent trial runs. For the sake of fair comparison, the initial population is kept identical between *Enhanced Imperialist Competition Algorithm*, EICA [21] and ABSICA in each run. Diversity tracing is a tool for studying behavior of algorithms [22–25]. A *Diversity Index,* DI is utilized as:

$$DI = \underset{q}{mean}\left(\frac{SD_q}{x_q^U - x_q^L}\right) \tag{10}$$

DI is defined as the normalized standard deviation averaged over the design variables using the original variable bounds x_q^L and x_q^U. The term SD_q stands for the standard deviation between individuals of the population in the q^{th} design variable. In the present work, parameters of adaptive variable band sizing are applied as $k = 10$ and $\alpha = 0.1$. A penalty factor of 10 is also used to avoid infeasible designs. Termination criterion in each example is set by total *NFE* .

Allowable Stress Design is applied in the present study for sizing design of pin-jointed structures due to AISC-ASD89 [26]; in which the stress limits are calculated as:

$$\begin{aligned}
&\sigma_{compression}^{allowable} = 0.6F_y \\
&\sigma_{compression}^{allowable} = \begin{cases} \dfrac{12\pi^2 E}{23\lambda^2} & , \dfrac{\lambda}{C_c} \geq 1 \\ (1-\dfrac{\lambda^2}{2C_c^{\,2}})F_y \Big/ (\dfrac{5}{3}+\dfrac{3}{8}\dfrac{\lambda}{C_c}-\dfrac{\lambda^3}{8C_c^{\,3}}), & \dfrac{\lambda}{C_c} < 1 \end{cases} \\
&C_c = \sqrt{2\pi^2 E \Big/ F_y}
\end{aligned} \tag{11}$$

where E denotes elasticity modulus and F_y stands for the yield stress. The slenderness factor of the corresponding member is denoted by λ. The stress constraints in this method is controlled by non-dimensional stress ratios as SR in the Eq. (1).

6.1 Design of 928-bar barrel-dome

Optimal design of a 928-bar barrel-dome structure is studied in this example. The problem was first introduced by the authors in continuous form [27]; however, it is treated here using discrete list of available sections as given in Table 1. This dome is a practical example of roof system for a sports' complex. A concentrated gravity load of 11 kN is applied at every node in the barrel part while each node in dome-part undergoes a vertical load of 5.5 kN. The structural members are distingushed in 7 groups by different ink in Fig. 2. The stress

[DOI: 10.22068/ijoce.2023.13.2.547]

constraint is controlled due to AISC-ASD89 provisions while the nodal displacement limit in each orthogonal direction is set to 0.05 m. The population size is taken 10.

Table 1. Available list of structural pipe sections

No.	Name		Area (cm^2)	Gyration radius (cm)
1	ST	½	1.613000	0.662432
2	EST	½	2.064512	0.635000
3	ST	¾	2.129028	0.846582
4	EST	¾	2.774188	0.818896
5	ST	1	3.161284	1.066038
6	EST	1	4.129024	1.034542
7	ST	1¼	4.322572	1.371346
8	ST	1½	5.161280	1.582166
9	EST	1¼	5.677408	1.331214
10	EST	1½	6.903212	2.003806
11	ST	2	6.903212	1.535430
12	EST	2	9.548368	1.945132
13	ST	2½	10.96772	2.416810
14	ST	3	14.38707	2.955798
15	EST	2½	14.51610	2.346452
16	DEST	2	17.16126	1.782572
17	ST	3½	17.29028	3.395726
18	EST	3	19.48383	2.882646
19	ST	4	20.45157	3.835908
20	EST	3½	23.74189	3.318002
21	DEST	2½	25.99995	2.143506
22	ST	5	27.74188	4.775454
23	EST	4	28.45156	3.749548
24	DEST	3	35.29025	2.658110
25	ST	6	35.99993	5.700014
26	EST	5	39.41928	4.675124
27	DEST	4	52.25796	3.490976
28	ST	8	54.19344	7.462012
29	EST	6	54.19344	5.577332
30	DEST	5	72.90308	4.379976
31	ST	10	76.77404	9.342628
32	EST	8	82.58048	7.309358
33	ST	12	94.19336	11.10361
34	DEST	6	100.6449	5.236464
35	EST	10	103.8708	9.216898
36	EST	12	123.8707	11.02893
37	DEST	8	137.4191	7.004812

[DOI: 10.22068/ijoce.2023.13.2.547]

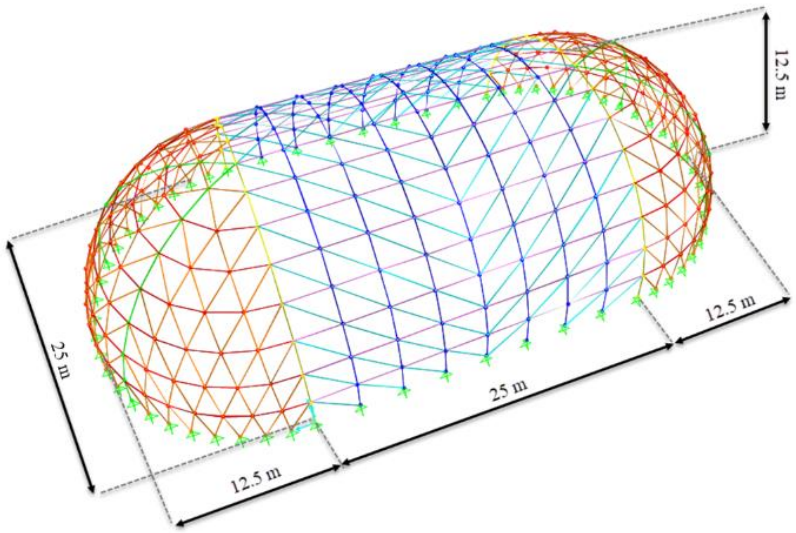

Figure 2. 928-bar barrel dome

Table 2. Results of sizing design for 928-bar barrel-dome example

Design Variable	EICA	ABSICA
X1	24	21
X2	13	16
X3	23	24
X4	37	24
X5	18	22
X6	23	18
X7	19	17
Best weight (kg)	79957.6	49723.4
Mean	92990.2	58062.3
SD	18430.1	11793.4
NFE	5000	5000

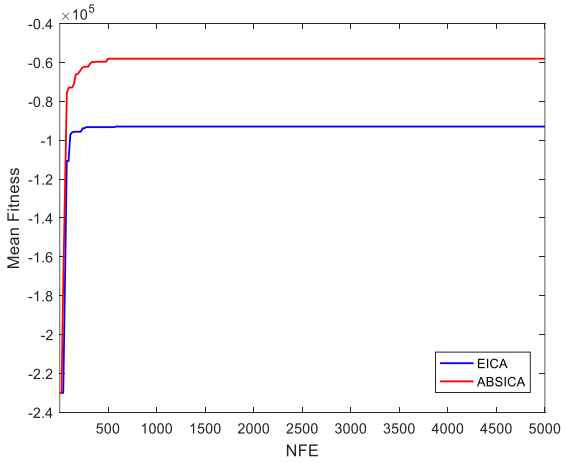

Figure 3. Convergence curves for the mean results of 928-bar design problem

[DOI: 10.22068/ijoce.2023.13.2.547]

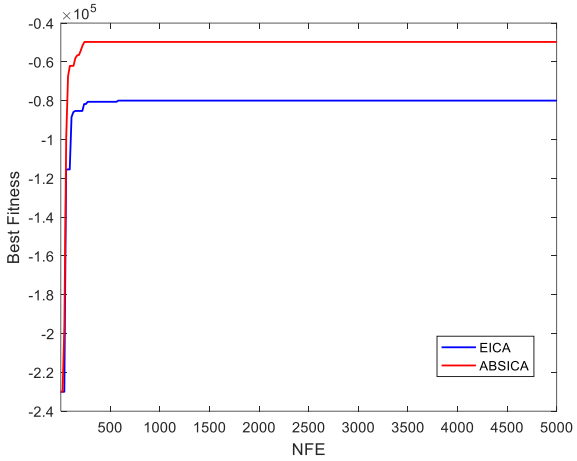

Figure 4. Convergence curves for the best results of 928-bar design problem

FORMIAN is a specialized software to assess complex architectural forms of space structures [28]. Appendix A.1 gives the FORMIAN code to genreate topology and geometry of this example. The lengths of rod members in the groups 1 to 7 are 2.45, 2.45, 2.45, 3.13, 3.97, 2.01 and 2.49 meters, respectively.

Convergence curves over independent trail runs are given in average by Fig. 3 and in the best run by Fig. 4. It is evident that the proposed strategy has led to considerable convergence improvement by ABSICA vs. EICA.

Quality of the final results and the corresponding statistics can be found in Table 2. EICA has decreased the structural weight up to 79957.6 kg; however, the best result of ABSICA is as least as 49723.4 kg. It is while the mean results show about 37% improvement due to the proposed adaptive band strategy in ABSICA with respect to EICA. Table 2 also declares superior performance of ABSICA over EICA regarding lower standard deviation.

Fig. 5 reveals band size history in the best optimization run for 7 design groups of the 928-bar design problem. It can be noticed that for most variables, both BS level and its fluctuations have shown rapid decrease via early iterations. The matter provides reasoning for higher convergence rate of ABSICA.

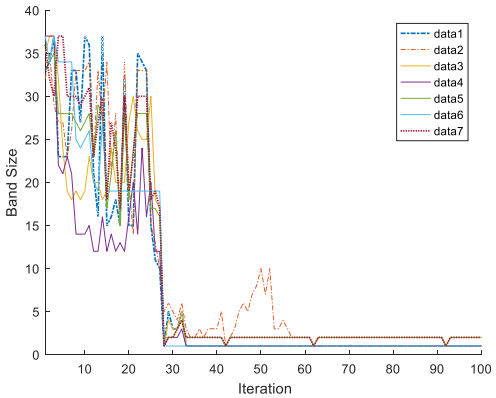

Figure 5. BS variation up to iteration 100 for 7 design variables in 928-bar truss design

[DOI: 10.22068/ijoce.2023.13.2.547]

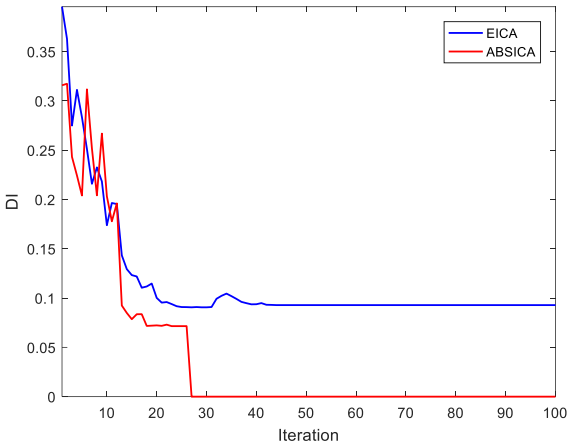

Figure 6. Diversity index history vs. iteration for 928-bar truss design

Another issue to study in this example; is the trend of diversity variation in the optimization process. According to Fig. 6, DI has experienced decreasing from 0.396 to nearly 0.100 by EICA but it is almost constant for further iterations. However, ABSICA continues on decreasing DI to approach zero. Such a diversity trace is in agreement with the history of BS variation in Fig. 5 to confirm higher convergence rate of ABSICA. Taking in mind that final results of ABSICA are better than EICA, it is concluded that the proposed strategy has provided better search refinement by such a trend of DI variation.

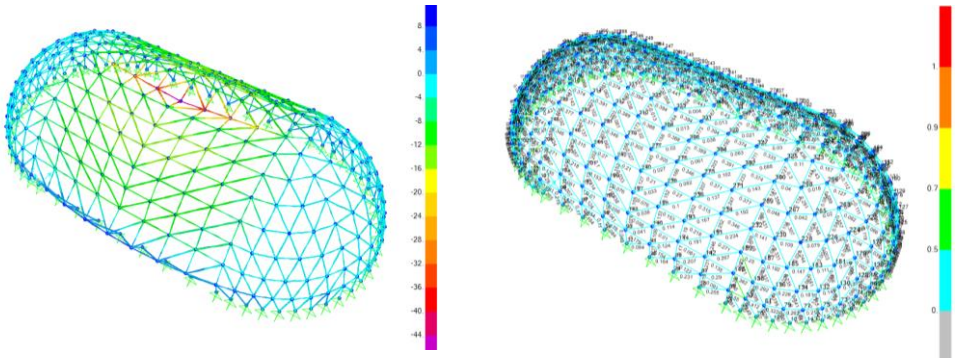

(a) (b)

Figure 7. Distribution of (a) deformation in meters and (b) stress ratios in the optimal design of 928-bar truss

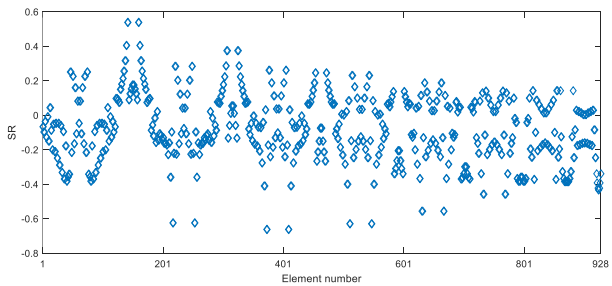

Figure 8. Member stress ratios of the optimal 928-bar truss

[DOI: 10.22068/ijoce.2023.13.2.547]

Maximum stress ratio of EICA design is obtained 0.404 over 928 elements while the displacements ratio over 353 nodes, is at most 0.942. Maximum stress and displacement ratios by ABSICA design are obtained as 0.539 and 0.998, respectively. The matter shows feasibility of the final design and activation of the displacement constraint in this example. Fig. 7 illustrates the deformed shape of the structure versus its unloaded shape. DR values have approached 1.00 exhibiting activation of the displacement constraint. Fig. 8 shows that the stress constraint is satisfied falling well below its limit of unity; however, not activated.

6.2 Design of 1512-bar symmetric dome

This example is treated to evaluate performance of the proposed algorithms in sizing design of a large-scale symmetric dome. Fig. 9 shows a 1512-bar dome truss with 408 nodes having a central upper ring and a lower ring of support nodes. The truss elements are divided into 9 symmetric groups. Considering 37 sections of Table 1 for each member group, cardinality of the search space is almost 1.3×10^{14}; that introduces a large-scale problem. Every node at the upper ring undergoes a load of 16 kN in the direction of gravity and 6 kN is vertically applied at the other free nodes. Material properties and stress constraints are the same as the previous example. The structure's geometry and topology are constructed using FORMIAN code given in Appendix A.2. The member lengths of the nine groups are 3.29, 3.29, 1.3, 2.96, 2.96, 2.11~5.15, 1.54~4.68, 3.31~3.54, and 2.63~3.24 meters, respectively. As can be realized some sizing groups include a variety of member lengths.

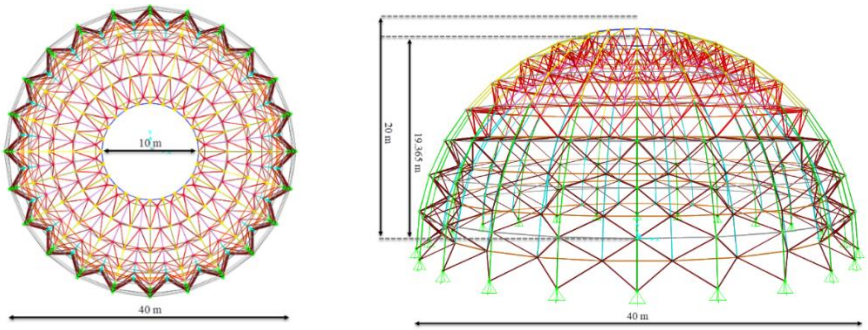

(a) (b)

Figure 9. 1512-bar dome truss: a) Top view, b) Side view

Statistical results for optimal designs of 1512-bar dome by the proposed methods are given in Table 3. The mean result of ABSICA for such a dome is obtained 27364.7 kg that is below 29841.4 kg by EICA; however, their best result shows 0.6% difference. Due to lower standard deviation, ABSICA has better robustness than EICA, in this example. Comparison of the convergence curves in Fig. 10; shows superiority of ABSICA in the mean results. According to Fig.11, the 9 design variables in this example, except the variables No.7 and No.8, exhibit general trend of decreasing BS in early iterations; that corresponds to high efficiency of ABSICA.

[DOI: 10.22068/ijoce.2023.13.2.547]

Table 3. Results of sizing design for 1512-bar dome truss

Design Variable	EICA	ABSICA
X1	15	21
X2	16	16
X3	35	32
X4	15	11
X5	17	10
X6	9	2
X7	4	12
X8	4	1
X9	1	3
Best weight (kg)	25203.9	25055.8
Mean	29841.4	27364.7
SD	3223.6	1843.4
NFE	5000	5000

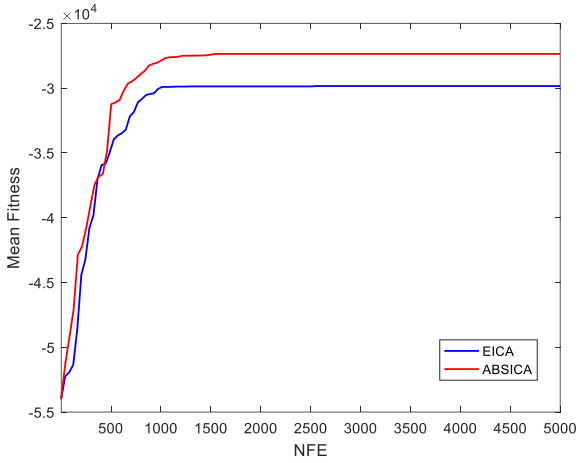

Figure 10. Convergence curves for the mean results of 1512-bar truss design

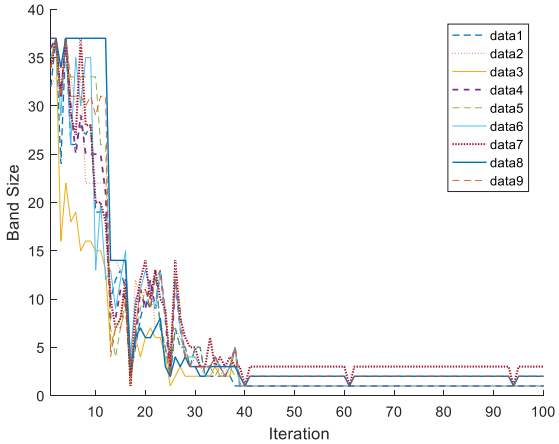

Figure 11. BS variation up to iteration 100 for the design variables in 1512-bar truss design

[DOI: 10.22068/ijoce.2023.13.2.547]

Such a trend is better studied by tracing DI in Fig. 12. Again, EICA shows nearly constant diversity after early iterations. It is while ABSICA has lowered such a level of diversity to provide better search refinement as the search progresses to the final iterations. However, it has not landed on zero diversity in such a more complex and large-scale problem. Higher fluctuation of DI trace in ABSICA with respect to EICA is also observed.

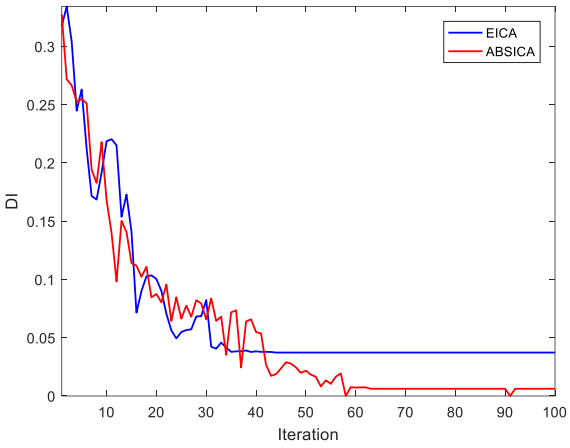

Figure 12. Diversity index history vs. iteration for 1512-bar truss design

Distribution of such deformation among the structural model is given by Fig. 13. The corresponding DR values are obtained 0.998 by EICA and 1.001 by ABSICA where the limit on the nodal displacement is taken 0.005 m. It is evident in Fig. 14 for such a design of the dome-shaped structure that the elements have taken certain SR values between -0.3 and 0.3. Based on AISC-ASD89, the maximum stress ratio has reached 0.235 by ABSICA while it is obtained 0.217 by EICA. Despite the stress limitation, the displacement constraint is activated by ABSICA in this example.

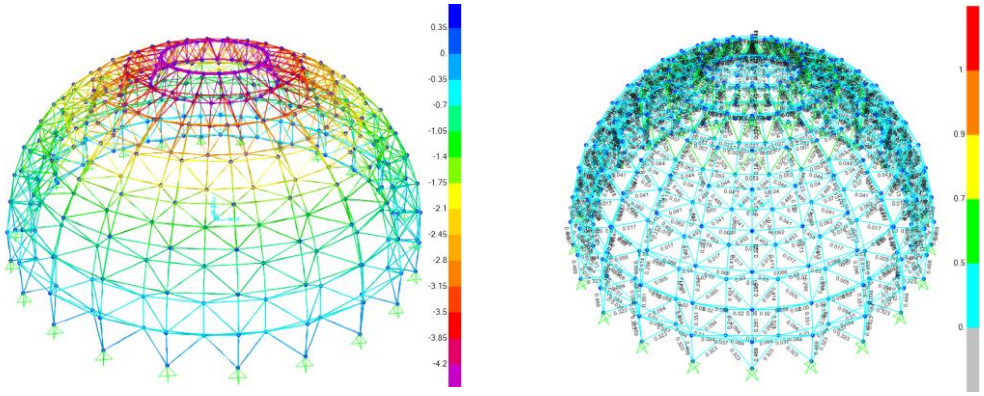

(a) (b)

Figure 13. Distribution of (a) deformation and (b) stress ratios in the optimal 1512-bar truss

[DOI: 10.22068/ijoce.2023.13.2.547]

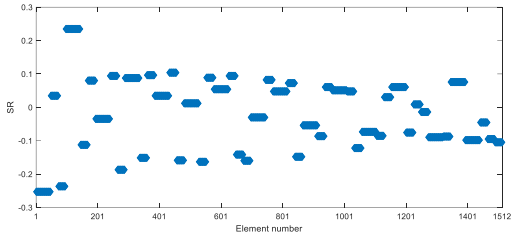

Figure 14. Member stress ratios of the optimal 1512-bar truss

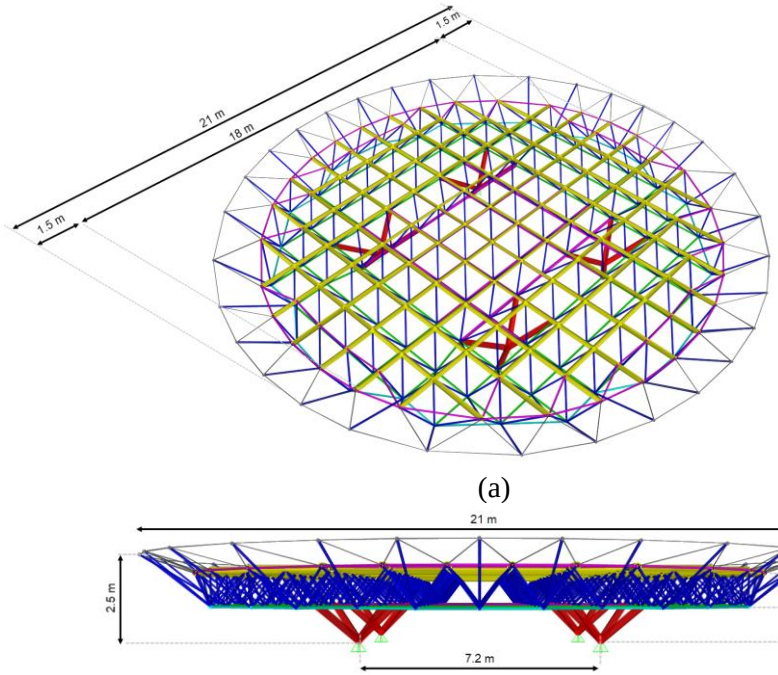

Figure 15. 1104-bar helipad truss: a) 3D view, b) Side view

6.3 Design of 1104-bar helipad structure

Helipad structures have many real-world applications such as in emergency buildings and hospitals, offshore structures and tall building towers [29]. Here, a steel helipad of Fig. 15 is considered to illustrate merit of the proposed algorithms in practical design. The problem has previously been formulated with continuous variables [30]; however in the present work, the sections are limited to be selected from the discrete list of Table 1. The structure contains two-layer grids with 1 m distance from each other. Diameter of the bottom layer is 18 m while the external diameter is 21 m. The structural members are embedded to the 9 sizing groups for which the member lengths are 1.50~1.73, 1.10~1.50, 1.50, 1.45~2.40, 1.50, 1.76~2.71, 1.50, 1.50~2.12, and 2.00 meters, accordingly.

In this structure, two load cases are applied to the top layer of the structure at the same time. The first one is the concentrated vertical load of 350 kgf applied at 4 central nodes and

[DOI: 10.22068/ijoce.2023.13.2.547]

the second applies the distributed load of 300 kgf/m^2 at all nodes of the top layer. The allowable tensile and compressive stresses are calculated due to the AISC-ASD89. Helipad has crucial functionality for which only small deformations are allowed. Hence, the displacements at every degree of freedom (in orthogonal directions) are limited here to 0.005 m; that is less than the span length divided by 240. The algorithms are run by 50 individuals and 20000 structural analyses in each independent run.

Convergence history of EICA and ABSICA are compared in Fig. 16. It is realized that in the mean results higher fitness is obtained by applying the proposed adaptive band strategy. According to Table 4, the best results of structural weight by the two methods are similar.

Fig. 17 reveals that distinct design variables have experienced more different and delayed trends of BS-decrease with respect to previous examples. The matter addresses the effect of structural shape and member grouping to resist its particular loading state.

Table 4. Results of sizing design for 1104-bar helipad example

Design Variable	EICA	ABSICA
X1	17	16
X2	23	25
X3	28	27
X4	12	12
X5	23	21
X6	1	1
X7	20	19
X8	15	11
X9	34	32
Best weight (kg)	24539.5	24420.9
Mean	24993.4	24745.3
SD	439.7	406.0
NFE	20000	20000

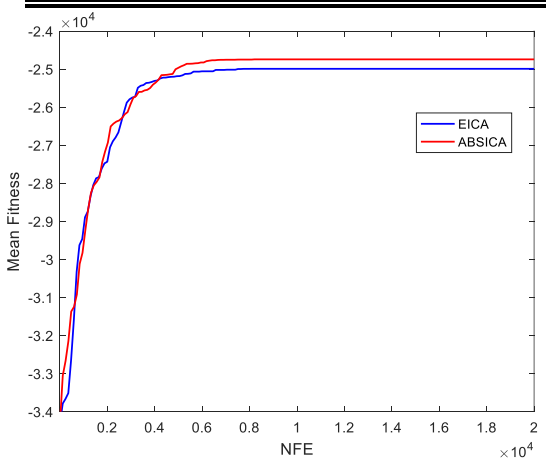

Figure 16. Convergence curves for the mean results of helipad design problem

In this practical example, final fitness improvement with respect to the fittest design in the initial population, is obtained 29%, showing a considerable merit in minimization of the construction material cost. DI traces in Fig. 18, better show behavior of the algorithms. It is observed that at the iterations where ABS subroutine is activated, the optimization process

[DOI: 10.22068/ijoce.2023.13.2.547]

experiences sudden diversity drops due to such local search. After that, it returns back to its general trend until next activation of ABS in the **Step 5** of ABSICA.

Fig. 19 gives a picture about distribution of deflection in the best optimal design by ABSICA. It can be realized due to location of supports, the structural responses are not in a full cycle symmetry; however, are observed in the mirrored parts about the orthogonal axes. The center part of helipad undergoes more reactions due to the applied loadings.

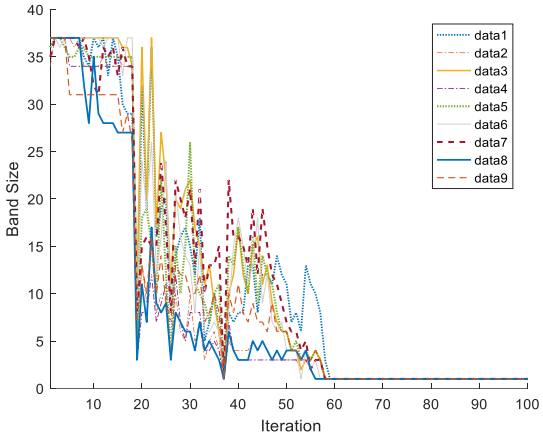

Figure 17. BS variation up to iteration 100 for the design variables in 1104-bar helipad design

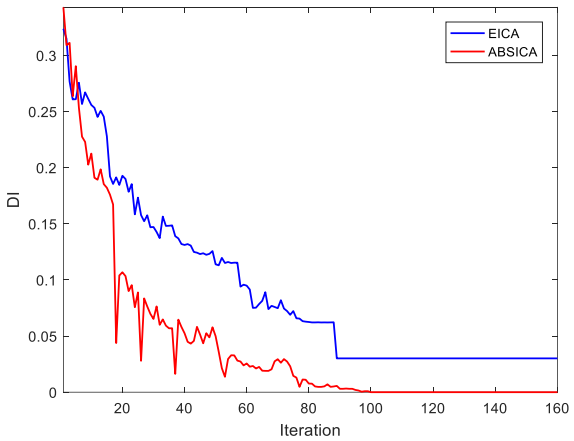

Figure 18. Diversity index history vs. iteration for 1104-bar helipad design

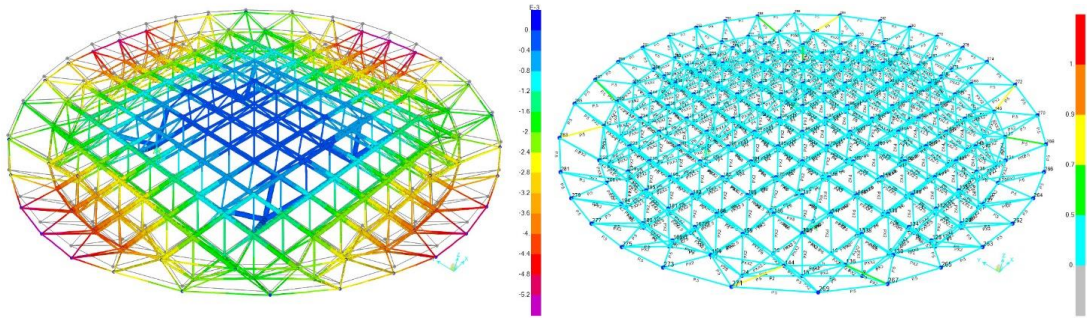

(a) (b)

Figure 19. Distribution of (a) deformation and (b) stress ratios in the optimal 1104-bar truss

[DOI: 10.22068/ijoce.2023.13.2.547]

According to Fig. 20, most helipad members are in a safe margin with the absolute SR less than 0.20; and a few members with more SR up to 0.36. This model has experienced more DR values up to 1.00. It shows capability of the proposed optimization algorithm to activate at least one type of the behavior constraints.

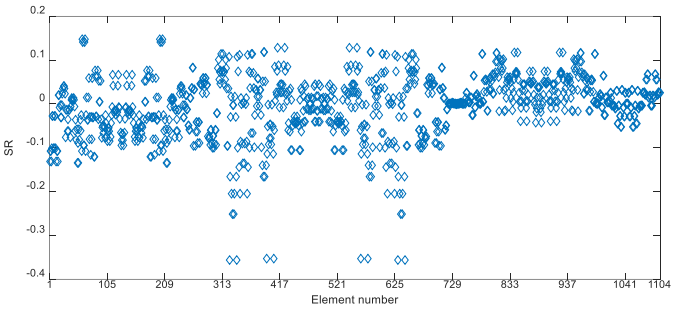

Figure 20. Member stress ratios of the optimal 1104-bar helipad truss design

7. CONCLUSION

The present study, has taken merit of orderable design spaces in discrete structural sizing due to the relation between member cross-section areas and total weight of the model. According to preliminary tests, it was found that the corresponding upper and lower limits on each design variable tend to concentrate on the optimal section index after some early fluctuations. The feature is accelerated via the proposed adaptive band strategy that works on a sorted section list and utilizes the history of BS variation. ABS has been designed to frequently tighten the band size for better refinement and again release it in order not to be trapped in local optima.

A hybrid PSO and ICA that takes advantages from operators of both, was selected to implement ABS. The proposed method was then applied on a number of space truss examples with various spatial shapes, to declare performance improvement in comparison with an enhanced variant of ICA. According to the results, the quality of optimal designs was improved in ABSICA with respect to the other method that does not apply ABS. In addition, better activation of constraints in the optimal point by ABSICA confirms its superior search refinement.

History of DI variation, declares how exploration and exploitation are balanced by the algorithms. It was observed that EICA stops DI decreasing after some early iterations. In the other hand, ABSICA enforces DI to decrease and drop into a much smaller level. Such a phenomenon is in agreement with the BS reduction for different variables; as a result of applying the adaptive-band strategy.

It is practical to fix the grouping for sizing design of a structure; especially when it is modular and in a particular spatial form. ABS relies on refinement of the band size for every variable rather than changing the number of such design variables. In this regard, the proposed method is an affordable solution for efficiency improvement in sizing design of

[DOI: 10.22068/ijoce.2023.13.2.547]

real-world structures with practical list of available sections.

APPENDIX

A.1. FORMIAN code of the 928-bar truss

```
S=25; (*) Span of barrel vault and the semi-domes (*)
H=12.5; (*) Rise of barrel vault and the semi domes (*)
L=25; (*) Length of barrel vault (*)
m=8; (*) Frequency of the semi-domes (*)
n=8; (*) Frequency along the
length of barrel vault, n must be even (*)
p=3; (*) Number of sectors of each semi-dome (*)
A=2*atan|(2*H/S); (*) Sweep angle (*)
R=S/(2*sin|A); (*) Circumradius (*)
E=rinit(2*m+1,n,1,1)|[1,0,0; 1,0,1]#
rinit(2*m,n-1,1,1)|[1,0,1; 1,1,1]#
lamit(m,n/2)|rinit(m,n/2,1,1)|
[1,1,0; 1,0,1];
B=verad(0,0,90-A)|bc(R,A/m,L/n)|E;
F=bd(R,180/p,A/m)|genit(1,m,1,1,0,1)|
{[1,0,0; 1,0,1], [1,0,0; 1,1,1],
[1,0,1; 1,1,1]};
D=pex|rosad(0,0,p,180/p)|F;
Domes=lam(2,-L/2)|D;
Barrel=verat(0,0)|B;
Bard=Barrel#Domes;
use &,vm(2),vt(2),
vh(2*R,2*R,8*R, 0,0,0, 0,0,1);
clear; draw Bard;
```

A.2. FORMIAN code of the 1152-bar truss

```
S=40; (*) Span of top layer (*)
P=10; (*) Gap diameter (*)
D=2; (*) Depth (*)
A=90; (*) Sweep angle (*)
m=24; (*) Frequency of
elements on a ring (*)
n=8; (*) Frequency of elements on a rib (*)
R=S/(2*sin|A); (*) Top radius (*)
Rb=R-D; (*) Bottom radius (*)
G=asin|(P/(2*R)); (*) Gap angle (*)
i=(A-G)/(2*n); (*) increment (*)
T=rinit(m,n+1,2,2*i)|[R,0,G; R,2,G]#
```


[DOI: 10.22068/ijoce.2023.13.2.547]

```
rinit(m,n,2,2*i)|[R,0,G; R,0,G+2*i];
B=rinit(m,n,2,2*i)|[Rb,1,G+i; Rb,3,G+i]#
rinit(m,n-1,2,2*i)|[Rb,1,G+i; Rb,1,G+3*i];
W=rinit(m,n,2,2*i)|lamit(1,G+i)|
[R,0,G; Rb,1,G+i];
Dome=bs(1,360/(2*m),1)|(T#B#W);
use &,vm(2),vt(2),vh(R,R,4*R, 0,0,0, 0,0,1);
clear; draw Dome;
```

REFERENCES

1. Vanderplaats GN. Structural optimization for statics, dynamics and beyond. J Brazilian Soc Mech Sci Eng 2006; **28**:316–22.
2. Mitchell AGM. The limits of economy of material in frame-structures. Philos Mag 1904; **8**:589–97.
3. Arora JS. Introduction to Optimum Design. London, UK: Elsevier; 2017.
4. Kaveh A, Bakhshpoori T. Metaheuristics: Outlines, MATLAB Codes and Examples. Springer International Publishing; 2019.
5. Kaveh A, Zakian P. Enhanced bat algorithm for optimal design of skeletal structures. Asian J Civ Eng 2014; **15**:179–212.
6. Kaveh A, Zolghadr A. A novel meta-heuristic algorithm: tug of war optimization. Int J Optim Civ Eng 2016; **6**:469–92.
7. Martínez P, Martí P, Querin OM. Growth method for size, topology, and geometry optimization of truss structures. Struct Multidiscip Optim 2007; **33**:13–26.
8. Kaveh A, Zolghadr A. Topology optimization of trusses considering static and dynamic constraints using the CSS. Appl Soft Comput 2013; **13**:2727–34.
9. Kaveh A, Zaerreza A. Shuffled shepherd optimization method: a new Meta-heuristic algorithm. Eng Comput 2020; **37**:2357–89.
10. Saka MP. Optimum Design of Pin-Jointed Steel Structures With Practical Applications. J Struct Eng 1990; **116**:2599–620.
11. Hasançebi O, Çarbaş S, Doğan E, Erdal F, Saka MP. Performance evaluation of metaheuristic search techniques in the optimum design of real size pin jointed structures. Comput Struct 2009; **87**:284–302.
12. Degertekin SO, Lamberti L, Ugur IB. Sizing, layout and topology design optimization of truss structures using the Jaya algorithm. Appl Soft Comput J 2018; **70**:903–28.
13. Lamberti L, Pappalettere C. Move limits definition in structural optimization with sequential linear programming. Part I: Optimization algorithm. Comput Struct 2003; **81**:197–213.
14. Kaveh A, Shahrouzi M. Simultaneous topology and size optimization of structures by genetic algorithm using minimal length chromosome. Eng Comput 2006; **23**:644–74.
15. Shahrouzi M, Kaveh A. Dynamic fuzzy-membership Optimization: an enhanced meta-heuristic search. Asian J Civ Eng 2015; **16**:249–68.
16. Dorigo M, Stützle T. Ant colony optimization. London, UK: The MIT press; 2016.
17. Hasançebi O, KazemzadehAzad S. Adaptive dimensional search: A new metaheuristic algorithm for discrete truss sizing optimization. Comput Struct 2015; **154**:1–16.

[DOI: 10.22068/ijoce.2023.13.2.547]

18. Eberhart R, Kennedy J. New optimizer using particle swarm theory. Proc. Int. Symp. Micro Mach. Hum. Sci., 1995, p. 39–43.
19. Atashpaz-Gargari E, Lucas C. Imperialist competitive algorithm: An algorithm for optimization inspired by imperialistic competition. 2007 IEEE Congr Evol Comput CEC 2007 2007:4661–7.
20. Okwu MO, Tartibu LK. Metaheuristic Optimization: Nature-Inspired Algorithms Swarm and Computational Intelligence, Theory and Applications. Springer International Publishing; 2020.
21. Shahrouzi M, Salehi A. Enhanced Imperialist Competitive Algorithm for Optimal Structural Design. Sci Iran 2020; **28**:1973–93.
22. Kaveh A, Zolghadr A. Truss optimization with natural frequency constraints using a hybridized CSS-BBBC algorithm with trap recognition capability. Comput Struct 2012; **102**–**103**:14–27.
23. Kaveh A, Zolghadr A. Comparison of nine meta-heuristic algorithms for optimal design of truss structures with frequency constraints. Adv Eng Softw 2014;**76**:9–30.
24. Shahrouzi M, Aghabaglou M, Rafiee F. Observer-teacher-learner-based optimization: An enhanced meta-heuristic for structural sizing design. Struct Eng Mech 2017; **62**:537–50.
25. Shahrouzi M, Kaveh A. An efficient derivative-free optimization algorithm inspired by avian life-saving manoeuvres. J Comput Sci 2022;**57**:101483.
26. AISC. Manual of Steel Construction: Allowable Stress Design. 9th ed. Chicago, Illinois: American Institute of Steel Constuction; 1989.
27. Shahrouzi M, Salehi A. Design of large-scale structures by an enhanced metaheuristic utilizing opposition-based Learning. 2020 4th Conf. Swarm Intell. Evol. Comput. CSIEC 2020, IEEE; 2020, p. 27–31.
28. Noushin H, Samavati O, Sazali A. Basics of Formian-K. 1st ed. www.formexia.com; 2016.
29. Krzymień W, Cieślak S. Initial Analysis of Helicopter Impact on Hospital Helipads. Trans Aerosp Res 2019; **2019**:14–23.
30. Shahrouzi M, Salehi A. Imperialist Competitve Learner-Based Optimization: a hybrid method to solve engineering problems. Int J Optim Civ Eng 2020; **10**:155–80.

[DOI: 10.22068/ijoce.2023.13.2.547]